

Generation and control of optical vortices using left-handed materials

Kevin J. Webb* and Ming-Chuan Yang

School of Electrical and Computer Engineering, Purdue University, 465 Northwestern Avenue, West Lafayette, Indiana 47907, USA

(Received 1 September 2005; revised manuscript received 28 February 2006; published 6 July 2006)

Optical vortices are shown to be generated in the near-field through interference between a propagating wave and the amplified evanescent field in a slab of lossy left-handed material. While small loss adversely impacts the sub-wavelength performance in the lens application, the vortex character shown relies on some degree of imperfection. These vortices can be controlled by means of gain/loss and the incident field.

DOI: 10.1103/PhysRevE.74.016601

PACS number(s): 42.30.Va, 42.25.Bs, 42.25.Fx, 78.20.Ci

Electromagnetic vortices have been shown to exist in a variety of linear [1–5] and nonlinear media [6,7]. Vortices are points or rings in space (in three dimensions) or points in a plane (lines along the dimension with no field variation, in two dimensions) of zero intensity (power density). Nomenclature such as dislocations and phase singularities have also been used to describe this phenomenon. The feature of the vortex is that the phase of the field increases or decreases by an integer multiple of 2π on a closed path encompassing the point or line [2].

Vortices have been found in simulations involving wave packets [1], monochromatic Gaussian beams [2,5], waveguides [3], and coupling through small apertures in a metal film [4]. They have been observed as solitons in nonlinear Kerr media [6], and black self-guided beams in Kerr media are an example [8]. They have also been seen in nonlinear semiconductor laser cavities, where they depend on the operating conditions [7]. A possible generation mechanism uses a phase mask which provides the 2π circumferential phase shift [9]. All of these vortex observations, with the exception of the subwavelength slit in a metal [4], have involved only propagating waves.

The advancing phase front around a vortex gives rise to circulating power flow, described by the Poynting vector \mathbf{S} or momentum of the wave. This field can impart a force to a particle, and can form an optical trap [9,10]. Such traps provide interesting opportunities for science and technology [9]. Vortices from a strong signal in a nonlinear Kerr medium can provide a guiding mechanism for a weaker signal [6]. Vortices have also been suggested as a means to null out a bright, coherent signal in order to achieve sensitivity to a low coherence background signal that could then be detected in the vortex [11].

Writing the phase of either the electric or magnetic field as ϕ , the topological quantum number or charge for the vortex is $s = \oint \nabla \phi \cdot d\mathbf{l} / (2\pi)$. Depending on the circulation, $s = \pm 1$. The sum of the topological number for all interactions has been shown to be conserved, and that birth requires the creation of two dislocations of opposite rotation [2,12].

We show that interference between propagating and evanescent fields can give rise to vortices in the neighborhood of a linear left-handed (LH) or negative refractive index slab. A LH medium provides evanescent field growth and a means to

achieve and control the vortices. The concept can be illustrated with a simple example. The superposition in free space of a z -propagating transverse electromagnetic (TEM) wave having electric field $\mathbf{E} = \exp(ik_0 z)\hat{\mathbf{y}}$, where k_0 is the free space wave number, and a transverse electric (TE) evanescent field with $\mathbf{E} = \cos(k_x x)\exp(-\alpha z)\hat{\mathbf{y}}$, with k_x the transverse phase constant and α the decay constant, will result in a nonzero curl of the Poynting vector \mathbf{S} and vortices rotating about the y direction. Generalizing, the superposition of propagating and evanescent fields can result in vortices. As the evanescent field is involved, such vortices would be generated in the near-field.

Veselago recognized some of the interesting properties of LH materials, one of which is negative refraction when a beam is incident on an interface [13]. Pendry suggested that a perfect lens or superlens could be achieved with a LH slab [14], based on the negative refraction of propagating waves and the amplification of decaying evanescent fields. Naturally, this prospect aroused great interest because of the many imaging applications which could benefit. With small conductor elements forming electric and magnetic dipoles operated beyond resonance, so-called metamaterials, negative refraction has been demonstrated in the microwave frequency range [15]. There have been many subsequent studies, including the use of photonic crystals to achieve negative refraction under some circumstances without being in an effective medium limit [16,17].

As the frequency approaches zero, the dielectric constant ϵ and relative permeability μ must be positive in order to have positive energy density. There must therefore be dispersion in these parameters with frequency. Given the real part, the imaginary or loss term is then dictated by the Kramers-Kronig relations, and vice versa [18]. These relations are based on the causal relationship between the field and the material dipole moment that it creates. With a simple dipole resonance model, negative ϵ and μ are achieved by operating at frequencies higher than the resonance. Hence, negative index materials must have some degree of loss, with fundamental implications on the decaying fields [19]. Any degree of loss will limit the amplified evanescent plane wave spectrum [19–22]. Also, mismatch in the lens material will adversely impact performance [23]. The use of gain has been proposed to compensate for the loss [22,24].

The ability of a LH slab to amplify evanescent fields leads us to propose its use as a means to generate near-field optical vortices. We use the LH slab geometry with thickness d in

*Email address: webb@purdue.edu

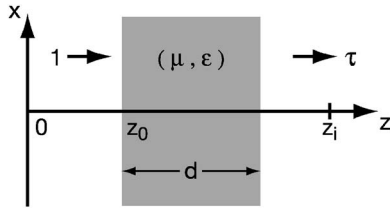


FIG. 1. Schematic of a left-handed (LH) slab lens showing the variables. The slab (shaded region) extends from z_0 to z_0+d . The object plane is $z=0$ and the image plane is $z=z_i$.

free space, as in Fig. 1. The object plane is $z=0$, the front surface of the slab is at $z=z_0$, and the image plane is at $z=z_i$. A perfect lens has $\mu=\epsilon=-1$, and the image plane occurs at $z_i=2d$. Consider the case of a low loss LH slab with $\epsilon=-1+i\epsilon'$ and $\mu=-1$, and a TM (H_y, E_x, E_z) evanescent field incident at $z=0$ with z dependence $\exp(-\alpha z)$, where $\alpha=\sqrt{k_x^2-k_0^2}$, with $k_0=2\pi/\lambda$ and λ the wavelength. The exact plane wave field transfer function is

$$\tau = \frac{(1-r^2)\exp(ik'_z d)}{1-r^2 \exp(2ik'_z d)} \exp(ik_z d), \quad (1)$$

where k_z (k'_z) denotes the z component of the wave vector in the RH (LH) medium and r is the reflection coefficient of the field incident onto the (semi-infinite) LH medium from the RH medium at $z=z_0$. For $(k_0/\alpha)^2\epsilon'' \ll 1$, the transfer function $\tau(z=2d)$ for the evanescent fields, from Eq. (1), can be approximated as [22]

$$\tau(z=2d) \approx \frac{\zeta}{1+\zeta}, \quad (2)$$

where $\zeta=\exp(-2\alpha d)/\Delta^2$, with $\Delta=(2+(k_0/\alpha)^2)\epsilon''/4$. For the lossless case, $\zeta \rightarrow \infty$ and $\tau(z=2d)=1$ for all evanescent fields,

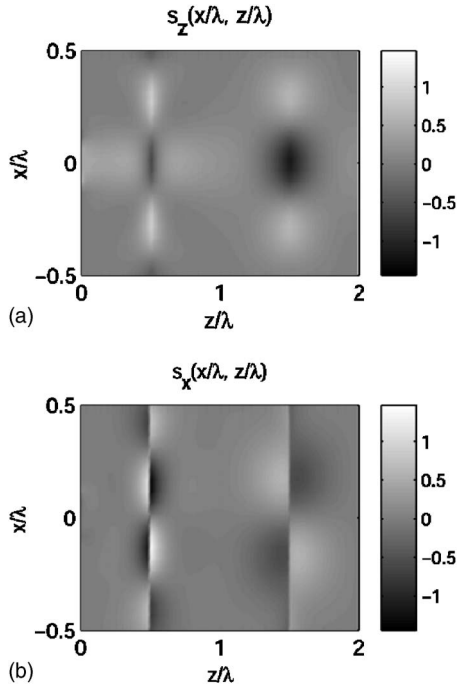


FIG. 2. Poynting vector for TM field incidence on a $d=\lambda$ LH slab ($z_0=0.5\lambda$, $\epsilon''=10^{-3}$): (a) S_z ; (b) S_x .

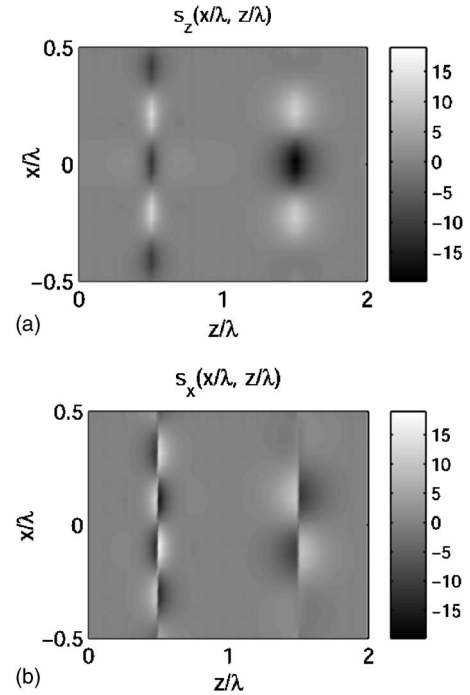


FIG. 3. Poynting vector for a TM incidence on a $d=\lambda$ LH slab ($z_0=0.5\lambda$, $\epsilon''=10^{-5}$): (a) S_z ; (b) S_x .

which allows the full reconstruction of the object at the image plane. The impact of small ϵ'' on the propagating fields is minor, whereas on the contrary, the evanescent spectrum can be severely impacted. This results in a truncated (or imperfect) plane wave transfer function. The band-limited evanescent spectrum can be amplified, and together with the propagating field, vortices can be formed.

Consider Fig. 1 as a lossy LH slab with $\epsilon=-1+i\epsilon''$ and $\mu=-1$. The fields in the object plane ($z=0$) can be expanded into a summation of plane wave components along the space-invariant transverse x direction. Since the behavior of each plane wave component in the geometry shown in Fig. 1 can be derived analytically, the corresponding electric field and magnetic field can be found. It is then sufficient to evaluate the time average Poynting vector, $\mathbf{S}(x, z)=(1/2)\text{Re}\{\mathbf{E} \times \mathbf{H}^*\}=S_x(x, z)\hat{\mathbf{x}}+S_z(x, z)\hat{\mathbf{z}}$, everywhere in Fig. 1, in order to investigate the vortex issue. We assume a TM field with

$$H_y(x, z=0) = \begin{cases} 1 & |x| < 0.1\lambda \\ 0 & \text{otherwise} \end{cases} \quad (3)$$

and then calculate \mathbf{S} everywhere for different values of ϵ'' in the LH slab. Figure 2 shows $\mathbf{S}(x, z)$ for a LH slab having $\epsilon''=10^{-3}$ and located between $z=0.5\lambda$ and $z=1.5\lambda$. The vortices can be observed as follows. At $z=1.5\lambda$, Fig. 2(a) shows negative S_z (power flowing backward) around $x=0$ and positive S_z (power flow forward) in the areas above and below. Figure 2(b) shows oppositely directed S_x on either side of the $z=1.5\lambda$ interface. While not visible on the scale in Fig. 2, vortices also occur at the image plane and elsewhere, with reducing amplitude as z/λ increases beyond the back surface of the slab. The image plane vortices disappear when the loss goes to zero. Notice also that the two vortices on the output

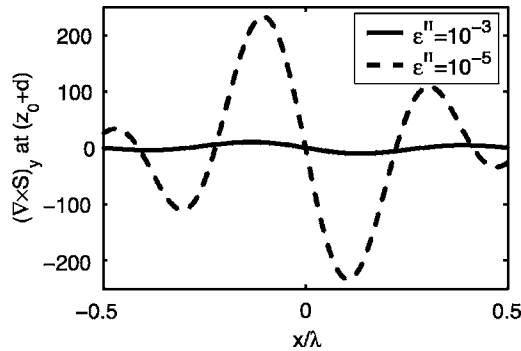


FIG. 4. The curl of the Poynting vector along the output surface of the slab ($z=z_0+d$) for the cases of Figs. 2 and 3.

face of the slab have opposite rotation, i.e., $s=1$ in one case and $s=-1$ in the other, consistent with the notion of creating vortices of opposite rotation [2,12]. Figure 3 shows the Poynting vector with the same geometry and incident field as for Fig. 2, but with $\epsilon''=10^{-5}$, i.e., with less loss. The sizes of the vortices are reduced, using, for example, a 3 dB measure. In this case, the increased bandwidth for τ provides for more rapid field variation and hence smaller vortex size. Figure 4 gives the curl of the Poynting vector at $z=z_0+d$ for the cases of Figs. 2 and 3 and shows changes in sign that confirm the presence of vortices.

Figure 5 shows S_z for a $d=\lambda$ slab with $z_0=0.5\lambda$ for three loss cases ($\epsilon''=10^{-3}, 10^{-4}, 10^{-5}$). The variation of S_z as a function of x becomes faster and the intensity larger as the loss decreases. The region where S_z is negative can be considered as a dark background, because an ideal detector which does not disturb the fields will not absorb photons in this region. This suggests that it would be possible to detect a weak signal located within the dark areas [11], or to determine the incoherent background noise from a measurement in these regions.

The results of Fig. 5 suggest that modifying the loss is a way to control the size and strength of a vortex. While this may occur by changing wavelength, due to dispersion, we describe an approach at fixed wavelength. Optical gain can be used to offset loss [22,24], and hence to control the vortices, even to turn them on and off. From Eq. (2), as τ is a function of ϵ''^2 , it suggests that for small values of $|\epsilon''|$ (either loss or gain), the spectrum of the amplified evanescent field

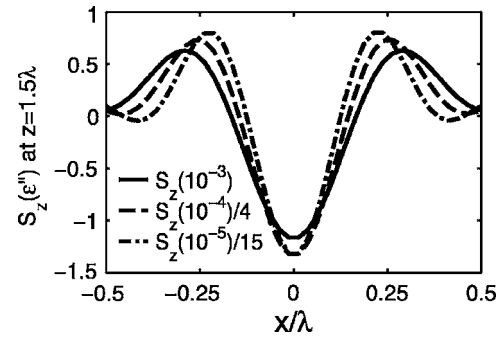


FIG. 5. The z component of the Poynting vector (S_z) at $z=1.5\lambda$ for different loss of the LH slab $\epsilon''=10^{-3}, 10^{-4}, 10^{-5}$.

will be approximately the same, under the assumption that $(k_0/\alpha)^2\epsilon'' \ll 1$. Suppose the LH slab can be realized with a gain material. The injected (pump) energy can then be used to either reduce the material loss or to reach net gain, in order to control the vortices.

The vortices we have shown for planar negative index slabs depend on loss and the incident field, and hence can be controlled by either varying the incident field or introducing gain. They occur with an incident field containing propagating and evanescent components. While loss in a LH lens restricts operation to the near-field, it also provides application opportunities through the generation of vortices. Control of loss, through gain, for example, allows control over the size and strength of the vortex. There is no fundamental restriction on the minimum vortex size, as the evanescent spectrum is involved, i.e., there is no restriction that they be limited by, or comparable to, the wavelength. The concept may thus be important in the nanophotonics field. Implementation would require use of metamaterials in an effective medium limit to achieve a negative refractive index [14,15].

Support came from the National Science Foundation (0203240-ECS and 0323037-ECS), the Army Research Office (DAAD 19-00-1-0387), and the Department of Energy Office of Nonproliferation and Research and Engineering (NA22), in conjunction with Lawrence Livermore National Laboratory.

[1] J. F. Nye and M. V. Berry, Proc. R. Soc. London, Ser. A **336**, 165 (1974).
[2] M. V. Berry, J. Mod. Opt. **45**, 1845 (1998).
[3] R. M. Jenkins, J. Banerji, and A. R. Davis, J. Opt. A, Pure Appl. Opt. **3**, 527 (2001).
[4] H. F. Schouten, T. D. Visser, D. Lenstra, and H. Blok, Phys. Rev. E **67**, 036608 (2003).
[5] M. V. Berry, J. Opt. A, Pure Appl. Opt. **6**, 259 (2004).
[6] G. A. Swartzlander and C. T. Law, Phys. Rev. Lett. **69**, 2503 (1992).
[7] J. Scheuer and M. Orenstein, Science **285**, 230 (1999).
[8] A. W. Snyder, L. Poladian, and D. J. Mitchell, Opt. Lett. **17**, 789 (1992).
[9] J. E. Curtis and D. G. Grier, Phys. Rev. Lett. **90**, 133901 (2003).
[10] K. T. Gahagan and G. A. Swartzlander, J. Opt. Soc. Am. B **16**, 553 (1999).
[11] G. A. Swartzlander, Opt. Lett. **26**, 497 (2001).
[12] J. F. Nye, J. Opt. A, Pure Appl. Opt. **5**, 495 (2003).
[13] V. G. Veselago, Sov. Phys. Usp. **10**, 509 (1968).
[14] J. B. Pendry, Phys. Rev. Lett. **85**, 3966 (2000).
[15] R. A. Shelby, D. R. Smith, and S. Schultz, Science **292**, 77

(2001).

- [16] C. Luo, S. G. Johnson, J. D. Joannopoulos, and J. B. Pendry, *Phys. Rev. B* **65**, 201104(R) (2002).
- [17] C. Luo, S. G. Johnson, J. D. Joannopoulos, and J. B. Pendry, *Opt. Express* **11**, 746 (2003).
- [18] J. D. Jackson, *Classical Electrodynamics*, 3rd ed. (Wiley, New York, 1999).
- [19] K. J. Webb, M. Yang, D. W. Ward, and K. A. Nelson, *Phys. Rev. E* **70**, 035602(R) (2004).
- [20] M. Nieto-Vesperinas, *J. Opt. Soc. Am. A* **21**, 491 (2004).
- [21] V. A. Podolskiy and E. E. Narimanov, *Opt. Lett.* **30**, 75 (2005).
- [22] M. Yang and K. J. Webb, *Opt. Lett.* **30**, 2382 (2005).
- [23] D. R. Smith, D. Schurig, M. Rosenbluth, S. Schultz, S. A. Ramakrishna, and J. B. Pendry, *Appl. Phys. Lett.* **82**, 1056 (2003).
- [24] S. A. Ramakrishna and J. B. Pendry, *Phys. Rev. B* **67**, 201101(R) (2003).